Proceedings of ASME FEDSM'03
4^{th} ASME_JSME Joint Fluids Engineering Conference
Honolulu, Hawaii, USA, July 6-10, 2003

FEDSM2003-45332

SCALING PROPERTIES IN ROTATING HOMOGENEOUS TURBULENCE

P.K. Yeung*and Jia Xu
School of Aerospace Engineering
Georgia Institute of Technology
Atlanta, Georgia 30332
Email: yeung@peach.ae.gatech.edu

K.R. Sreenivasan
Institute for Physical Science and Technology
University of Maryland
College Park, MD 20742
Email: sreeni@ipst.umd.edu

ABSTRACT

The effects of uniform solid-body rotation on the scaling properties of turbulent flow (considered in a rotating frame) are studied by direct numerical simulation at two rotation rates, with a focus on the statistics of the velocity field including velocity gradients, enstrophy and energy dissipation rate. Especially at the high rotation rate, there is substantial evidence for anisotropy at the small scales, for reduced likelihood of extreme events in both enstrophy and dissipation (whose statistics become somewhat alike), and for the failure of classical Kolmogorov scaling in this flow.

NOMENCLATURE

Ro_T Initial turbulent Rossby number
$T_{E,0}$ Initial eddy-turnover time
$\langle\cdot\rangle$ Ensemble average
σ^2 Variance (mean-squared fluctuation)
μ_3 Skewness factor
μ_4 Flatness factor
$D_{LL}(r)$ Second-order longitudinal velocity structure function
$D_{LLL}(r)$ Third-order longitudinal velocity structure function

INTRODUCTION

Turbulence subjected to solid-body rotation arises in many important applications such as turbomachinery with rotating blades in engineering, and large-scale geophysical flows affected by the rotation of the Earth. Speziale [1] recognized that most classical turbulence models and theories must be modified to account for the distinctive effects of rotation resulting from the addition of Coriolis forces to the equation of motion. It is well known that rotation tends to reduce the energy cascade from the large scales to the small scales. Because this cascade is a fundamental characteristic of nonlinear scale interactions in three-dimensional turbulent flow, one can expect that classical scaling properties viewed in the context of Kolmogorov phenomenology are also substantially modified. For instance, Zhou [2] has proposed that the inertial-range energy spectrum would vary with wavenumber as k^{-2}. However, the current understanding of this subject is still essentially qualitative, and there is little information in the literature concerning how key statistical properties such as the non-Gaussianity at small scales are modified by rotation. Experimental work is also hampered by difficulties in laboratory set-up, although recent innovations in the use of liquid helium (e.g., Bewley *et al.* [3]) allowing compact-size apparatus are showing significant promise.

In this paper we follow the approach of Yeung & Zhou [4] in using direct numerical simulation (DNS) to examine the structure of rotating turbulence evolving from isotropic initial conditions. Our main objective here is to study the statistical characteristics of several important flow variables, including the velocity, velocity gradients, strain rates, vorticity components as well as energy dissipation and enstrophy. Because rotation reduces the spectral cascade, and promotes a tendency towards two-dimensionality, it is reasonable to suggest that rotation will tend to reduce intermittency at the small scales. We present numerical results from DNS

*Address all correspondence to this author.

which confirm this physical picture. Considerable contrasts with non-rotating turbulence are also observed in the properties of velocity structure functions and statistics of two-point velocity differences. It should be noted that the present results are for forced turbulence with statistically isotropic initial conditions, whereas the case of decaying turbulence is also of interest ([3], [5], [6]).

OVERVIEW OF NUMERICAL SIMULATIONS

We consider numerical solutions of the Navier-Stokes equations for the velocity in a frame rotating at constant rate $\underline{\Omega}$, written in tensor form as

$$\frac{\partial u_i}{\partial t} + u_j \frac{\partial u_i}{\partial x_j} = -\frac{1}{\rho}\frac{\partial p}{\partial x_i} - 2\varepsilon_{ijk}\Omega_j u_k + \nu \frac{\partial^2 u_i}{\partial x_j \partial x_j} + f_i, \quad (1)$$

where f_i represents numerical forcing applied to the large scales. The axis of rotation is chosen to be the x_3 (or z) direction (with $\Omega_j = \Omega\delta_{3j}$), which implies a state of statistical axisymmetry can be expected in the orthogonal (x-y) plane. Numerical methods used are the same as in [4], namely the pseudo-spectral algorithm of Rogallo [7] for homogeneous turbulence modified to allow the linear Coriolis term to be integrated exactly (Mansour *et al.* [8]). The latter modification is important in allowing simulations at high rotation rates without further limitations on the time step size in an explicit second-order Runge-Kutta scheme.

Although our eventual goal is to cover a wider parameter range, as in [4] we present results for one initial Reynolds number and two rotation rates (Ω). The turbulent Rossby number $Ro_T = \langle\varepsilon\rangle/(2K\Omega)$ is used to compare the time scale of rotation ($1/\Omega$) to that of the large eddies ($\langle\varepsilon\rangle/2K$, where K is the turbulence kinetic energy and $\langle\varepsilon\rangle$ is the dissipation rate). Because rotation causes the spectrum to shift towards the large scales which have relatively few samples in a domain of finite size, to ensure statistical accuracy we have performed ensemble averaging over the results of multiple independent realizations of the flow. We have six realizations for each rotation rate, compared to two in [4] for the higher rotation rate. Initial conditions correspond to forced isotropic turbulence of the type documented in [9], at an initial Taylor-scale Reynolds number about 140, which is just sufficient to show the beginnings of an inertial range in the energy spectrum of non-rotating isotropic turbulence.

To verify consistency with previous work we first show in Figure 1 the evolution of K and $\langle\varepsilon\rangle$ in time for both rotation rates, at $Ro_T = 0.0195$ and 0.0039 based on initial values of K and $\langle\varepsilon\rangle$, with time t normalized by the eddy-turnover time of the large scale motions based on the initial conditions. We shall refer to these two cases as "low rotation" and "high rotation", respectively. In both cases, as found in [4], both K and $\langle\varepsilon\rangle$ decay initially before energy input by forcing becomes effective, whereas at later times the kinetic energy increases and the dissipation remains nearly constant. This behavior is symptomatic of reduced energy transfer from the large scales to the small scales, which can be demonstrated explicitly by detailed spectral transfer calculations.

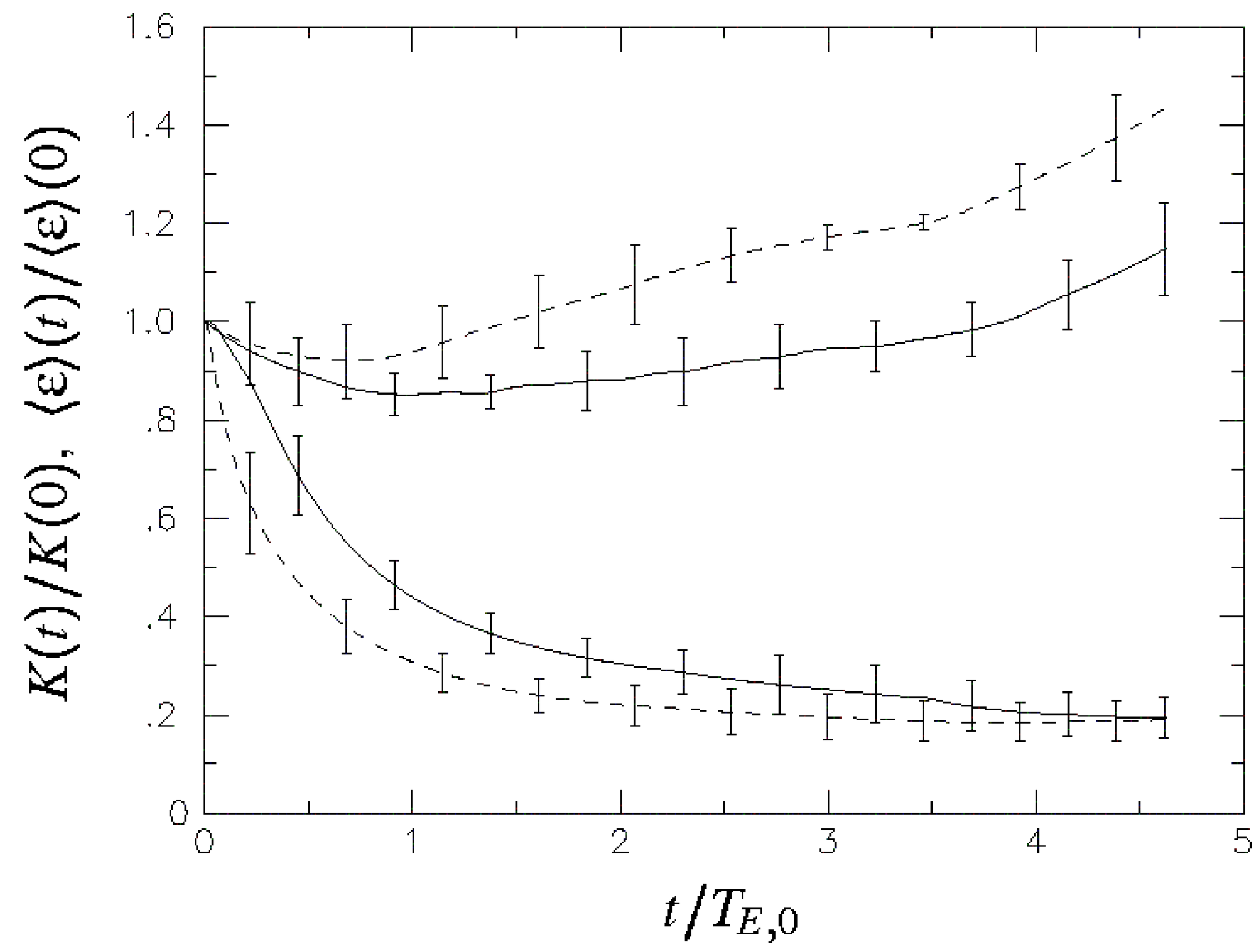

Figure 1. EVOLUTION OF TURBULENCE KINETIC ENERGY (UPPER CURVES) AND DISSIPATION RATE (LOWER CURVES) NORMALIZED BY INITIAL VALUES. VERTICAL LINES INDICATE 95% CONFIDENCE INTERVALS. SOLID LINES AND DASHED LINES FOR LOW AND HIGH ROTATION RATES RESPECTIVELY.

RESULTS FROM DATA ANALYSIS

We present new results based on analysis of the DNS database of instantaneous velocity fields archived at time intervals of order one initial eddy-turnover time. Quantities reported below include single-point moments, probability density functions, and structure functions representing moments of velocity differences between two points in space. Averages are taken over space, over the ensemble of six realizations for each rotation rate, and over the x and y components in the orthogonal plane where appropriate. As noted earlier, our primary focus is to characterize the effects of rotation on local isotropy (or anisotropy) and intermittency at small scales.

Velocity and Velocity Gradients

It is known from previous work ([4]) that the variances of all velocity component under rotation remain of the same order of magnitude, as in the non-rotating case; however, the fluctuating gradients along the axis of rotation (z) become small compared to the other two. Table 1 shows information on normalized third- and fourth order moments of velocity and longitudinal velocity gradients (i.e., their skewness and flatness factor, μ_3

and μ_4, respectively). There are some indications that the velocity becomes sub-Gaussian, but a serious confirmation requires longer simulations. On the other hand, it is clear that strong rotation causes the longitudinal velocity gradients to lose their skewness (which is typically about -0.5 in non-rotating isotropic turbulence). The flatness factor also decreases, especially for $\partial w/\partial z$ measured along the axis of rotation. This suggests a reduction of extreme events, as measured by departures from Gaussian behavior in one-point probability distributions.

Table 1. MOMENTS OF VELOCITY AND LONGITUDINAL VELOCITY GRADIENTS AT DIFFERENT TIMES.

$Ro_T = 0.0195$ (low rotation)				
$t/T_{E,0}$	1.22	2.44	3.66	4.87
μ_4 of u, v, w	2.91	2.92	2.68	2.54
μ_3 of $\partial u/\partial x$, $\partial v/\partial y$	-0.25	-0.19	-0.18	-0.16
μ_4 of $\partial u/\partial x$, $\partial v/\partial y$	3.97	4.19	4.45	4.71
μ_3 of $\partial w/\partial z$	-0.38	-0.32	-0.29	-0.26
μ_4 of $\partial w/\partial z$	4.33	5.19	5.52	6.59
$Ro_T = 0.0039$ (high rotation)				
$t/T_{E,0}$	1.22	2.44	3.66	4.87
μ_4 of u, v, w	2.86	2.84	2.81	2.60
μ_3 of $\partial u/\partial x$, $\partial v/\partial y$	-0.05	-0.05	-0.04	-0.01
μ_4 of $\partial u/\partial x$, $\partial v/\partial y$	3.05	3.23	3.64	3.65
μ_3 of $\partial w/\partial z$	-0.03	-0.01	-0.03	-0.02
μ_4 of $\partial w/\partial z$	3.04	3.04	3.06	3.03

Moments of the transverse velocity gradients and vorticity components are given in Table 2. In locally isotropic turbulence the statistics of all six transverse velocity gradients would be equivalent. However, it can be seen that rotation induce systematic (albeit modest) differences among transverse gradients wholly in the orthogonal plane, transverse gradients of the spanwise velocity, and spanwise gradients of transverse velocity components. In particular it is clear that, together with the data in Table 1, gradients taken in the spanwise direction become Gaussian-like under strong rotation. At the same time, the spanwise vorticity (ω_z) appears to be slightly less non-Gaussian than the other two components (ω_x, ω_y). We also observe that, as rotation effects become more established at later times, spanwise vorticity fluctuations (measured in the rotating frame) become smaller compared to those in the orthogonal plane. This is consistent with a trend for the fluid to begin to rotate increasingly like a solid body, with a more uniform rotation rate (which is subtracted off when we compute statistics in a rotating frame).

In both Tables 1 and 2 it may be noted also that the flatness factors listed are generally lower than those found for non-rotating turbulence at comparable Reynolds number (see, e.g. [10]). This again indicates that rotation tends to reduce rare events.

Table 2. TRANSVERSE VELOCITY GRADIENTS AND VORTICITY COMPONENTS.

$Ro_T = 0.0195$				
$t/T_{E,0}$	1.22	2.44	3.66	4.87
μ_4 of $\partial u/\partial y$, $\partial v/\partial x$	5.02	5.13	5.43	5.59
μ_4 of $\partial w/\partial x$, $\partial w/\partial y$	5.43	5.99	6.32	6.25
μ_4 of $\partial u/\partial z$, $\partial v/\partial z$	4.58	5.05	5.94	7.08
$\langle\omega_z^2\rangle/\frac{1}{2}[\langle\omega_x^2\rangle+\langle\omega_y^2\rangle]$	1.31	1.29	1.23	1.15
μ_3 of ω_x, ω_y	0.00	-0.06	-0.08	-0.03
μ_3 of ω_z	0.38	0.45	0.53	0.49
μ_4 of ω_x, ω_y	4.83	5.53	5.98	6.07
μ_4 of ω_z	4.19	4.36	4.53	4.63
$Ro_T = 0.0039$				
$t/T_{E,0}$	1.22	2.44	3.66	4.87
μ_4 of $\partial u/\partial y$, $\partial v/\partial x$	3.34	3.66	4.67	4.41
μ_4 of $\partial w/\partial x$, $\partial w/\partial y$	3.87	4.89	5.29	5.17
μ_4 of $\partial u/\partial z$, $\partial v/\partial z$	3.03	3.02	2.99	3.06
$\langle\omega_z^2\rangle/\frac{1}{2}[\langle\omega_x^2\rangle+\langle\omega_y^2\rangle]$	1.07	0.90	0.78	0.65
μ_3 of ω_x, ω_y	0.02	-0.09	-0.11	-0.16
μ_3 of ω_z	0.12	0.14	0.20	0.21
μ_4 of ω_x, ω_y	3.33	3.97	4.41	4.52
μ_4 of ω_z	3.14	3.41	4.24	4.13

Enstrophy and Dissipation

A question that often arises in the description of small-scale statistics is whether the enstrophy (square of vorticity, as $\omega^2 = \omega_i\omega_i$) is more intermittent than the energy dissipation rate ($\varepsilon = 2\nu s_{ij}s_{ij}$, based on the fluctuating strain rates, s_{ij}). In most of the DNS literature (e.g., [11], [12]) enstrophy is found to be more intermittent than dissipation, but it has been argued that the difference may vanish in the limit of high Reynolds number (e.g., [13], [14]). Because of the close connection between rotation and vorticity, it seems likely that the enstrophy would be modified more strongly by rotation than dissipation.

Table 3 shows the basic statistical moments of ω^2 and ε. Skewness and flatness factors for both of these quantities are lower than those in non-rotating turbulence (e.g. $\mu_3 \approx 8.9$ for ω^2, 4.9 for ε at a Reynolds number corresponding to the initial conditions). At low rotation enstrophy continues to possess larger skewness and flatness factors, but, at high rotation, the skewness and flatness factors for ω^2 and ε become essentially identical. However, the variance of $\ln\omega^2$, which is often thought to be a measure of intermittency, remains larger than that of $\ln\varepsilon$. This result may seem somewhat surprising and certainly requires further investigation.

Table 3. ENSTROPHY AND DISSIPATION.

$Ro_T = 0.0195$				
$t/T_{E,0}$	1.22	2.44	3.66	4.87
μ_3 of ω^2	5.08	6.25	5.70	6.61
μ_4 of ω^2	70.1	143.7	88.6	137.9
μ_3 of ε	4.27	5.56	5.31	5.82
μ_4 of ε	43.0	93.9	67.7	88.6
$\sigma^2_{\ln\omega^2}/\sigma^2_{\ln\varepsilon}$	1.64	1.57	1.51	1.47
$Ro_T = 0.0039$				
$t/T_{E,0}$	1.22	2.44	3.66	4.87
μ_3 of ω^2	2.28	3.44	3.90	4.05
μ_4 of ω^2	13.4	26.3	34.7	30.0
μ_3 of ε	2.22	3.52	4.01	4.16
μ_4 of ε	14.5	27.5	35.2	30.7
$\sigma^2_{\ln\omega^2}/\sigma^2_{\ln\varepsilon}$	1.83	1.67	1.59	1.49

Velocity Structure Functions

The behavior of velocity structure functions plays a central role in the original formulation of similarity hypotheses by Kolmogorov [15]. The m-th order longitudinal structure function is defined as the m-th order moment of the difference in a selected velocity component measured at two points a distance r apart along the same coordinate axis. If the distance r falls into the inertial range, i.e. $\eta \ll r \ll l$ (where η is the Kolmogorov length scale and l is a large-eddy length scale) then classical results for the longitudinal structure functions of second and third order are

$$D_{LL}(r) = C_2 \langle\varepsilon\rangle^{2/3} r^{2/3} \tag{2}$$

and

$$D_{LLL}(r) = -(4/5)\langle\varepsilon\rangle r\,. \tag{3}$$

Here $C_2 \approx 2.13$ in (2) is based on the use of isotropy relations and experimental data on the energy spectrum (Sreenivasan [16]), whereas (3) is exact. In rotating turbulence it is necessary to distinguish between results for r taken in directions parallel or perpendicular to the axis of rotation.

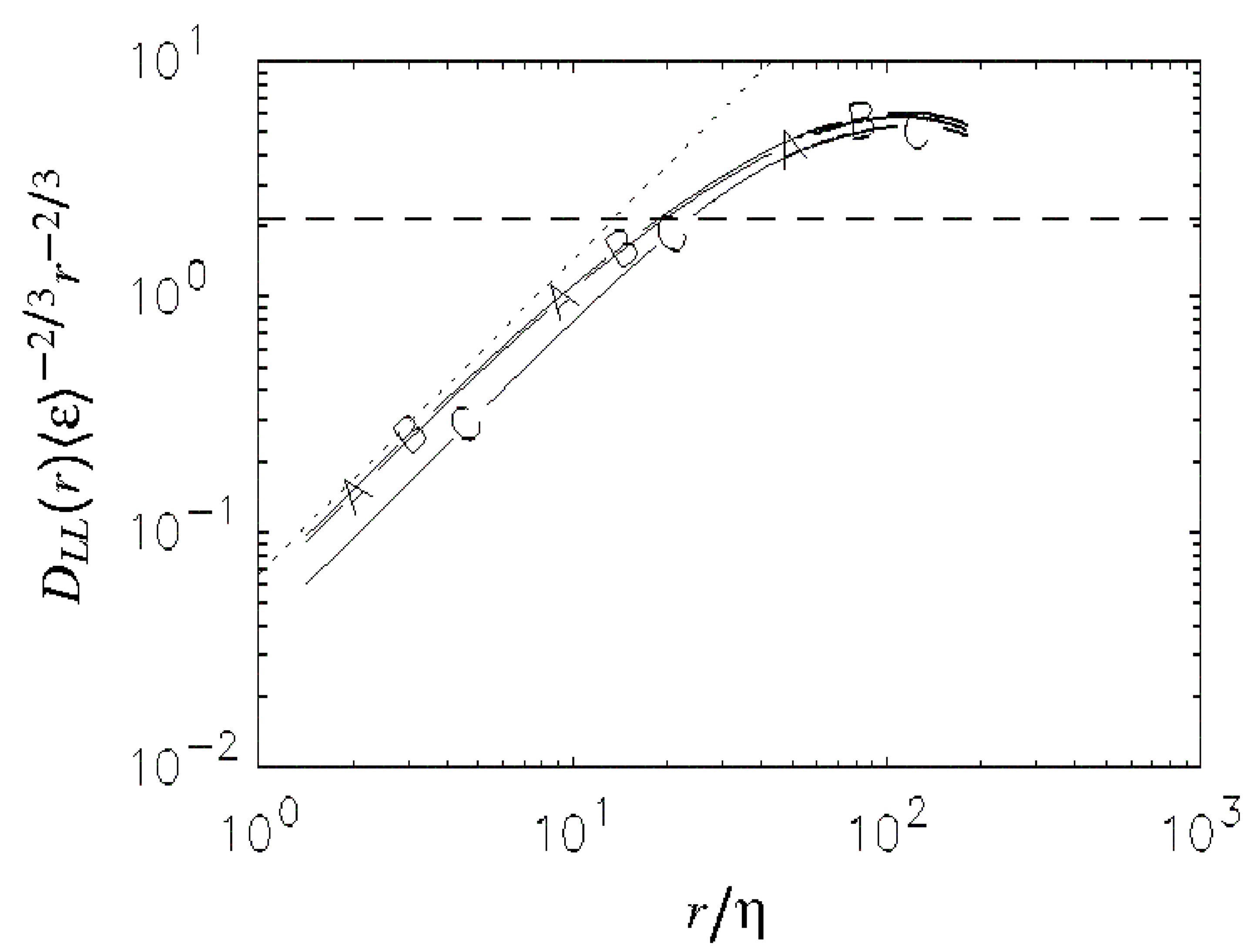

Figure 2. SECOND-ORDER STRUCTURE FUNCTIONS SCALED BY KOLMOGOROV VARIABLES, IN THE HIGH ROTATION CASE AT $t/T_{E,0} \approx 4.87$ FOR SPATIAL SEPARATIONS IN DIFFERENT COORDINATE DIRECTIONS (A,B,C FOR x,y,z COMPONENTS RESPECTIVELY). DOTTED AND DASHED LINES REPRESENT CLASSICAL SCALING FOR SMALL SCALES AND IN THE INERTIAL RANGE.

Figure 2 shows the behavior of the second-order structure function compared with classical Kolmogorov scaling, at a later time in the high-rotation run. For non-rotating isotropic turbulence the expected result at small r derived from the isotropic relation $\langle\varepsilon\rangle = 15\nu\langle(\partial u/\partial x)^2\rangle$ is illustrated by the dotted line at slope 1/3 for the normalized structure function, while data at intermediate r approach (from below) an inertial range plateau at height C_2 with increasing Reynolds number. It can be seen that rotation causes substantial deviations from the classical results.

At small r the second-order structure function is proportional to the mean-squared longitudinal velocity gradient, which is clearly smallest along the axis of rotation. At larger values of r there is a substantial overshoot, which implies that two-point correlations decrease less slowly with increasing scale separation, and is in turn consistent with the energy spectrum being shifted towards the low wavenumbers. The approximate isotropy at large r is also consistent with the velocity components (which are all dominated by the large scales) possessing root-mean-square values of the same order of magnitude.

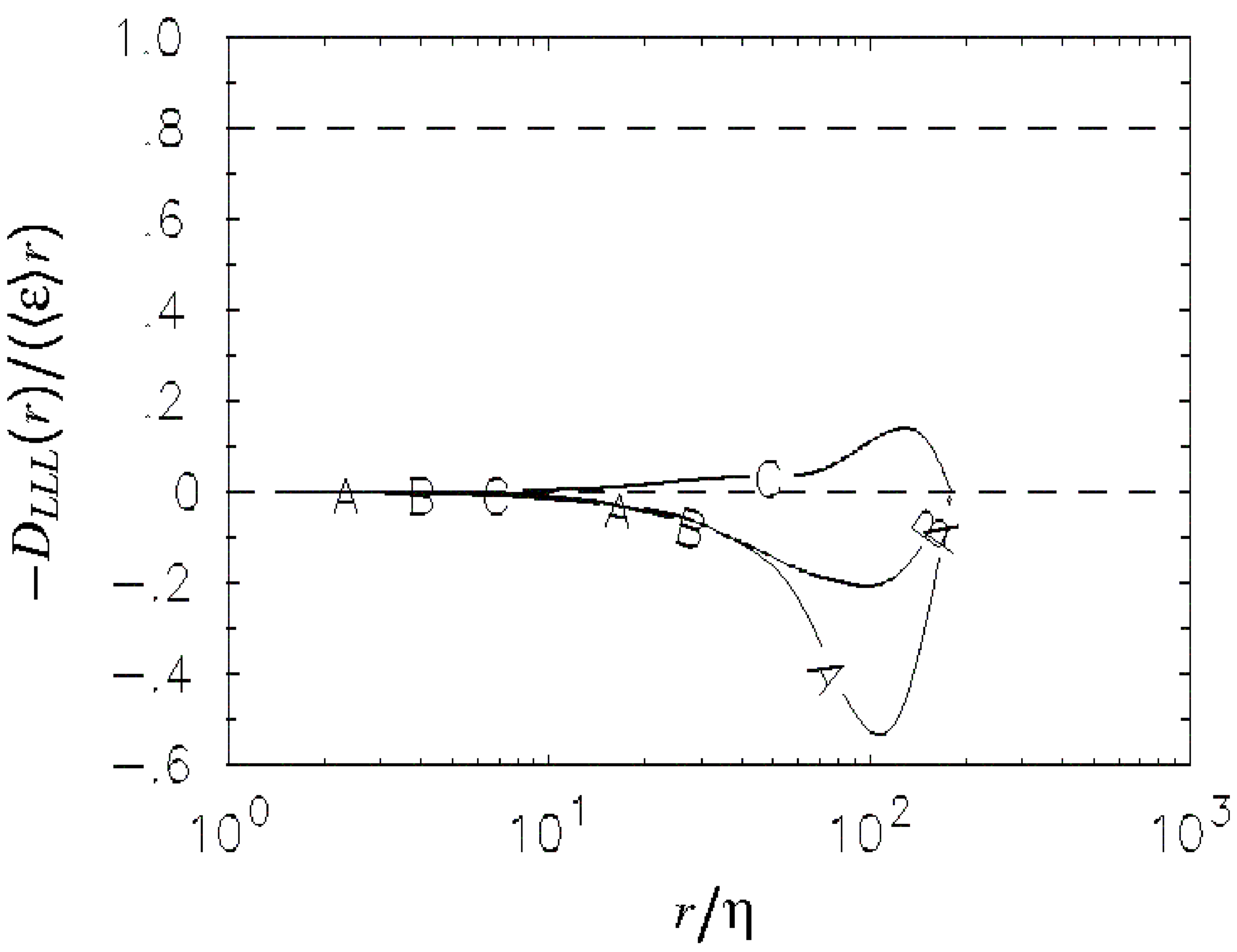

Figure 3. (NEGATIVE OF) THIRD-ORDER LONGITUDINAL STRUCTURE FUNCTIONS IN DIFFERENT DIRECTIONS SCALED BY KOLMOGOROV VARIABLES, UNDER THE SAME CONDITIONS AS FIGURE 2.

The large deviations seen in Figure 2 strongly suggest that the third-order structure function would not scale as Eq. 3, either. This is clearly seen in Figure 3, which has a dashed line drawn at height 0.8 for comparison. In addition, in Figure 4 we show the variation of skewness of the velocity increment u_r as a function of scale size r in different directions. Theoretical values for isotropic turbulence at high Reynolds number are about -0.5 at small r (corresponding to the velocity gradient $\partial u/\partial x$), and about -0.257 in the inertial range (based on Eqs. 2 and 3). In contrast, it can be seen that under strong rotation the skewnesses in all three directions and for all values of r are small and may be treated as effectively zero.

CONCLUSIONS

In this paper we have used direct numerical simulations of forced and homogeneous rotating turbulence with initially

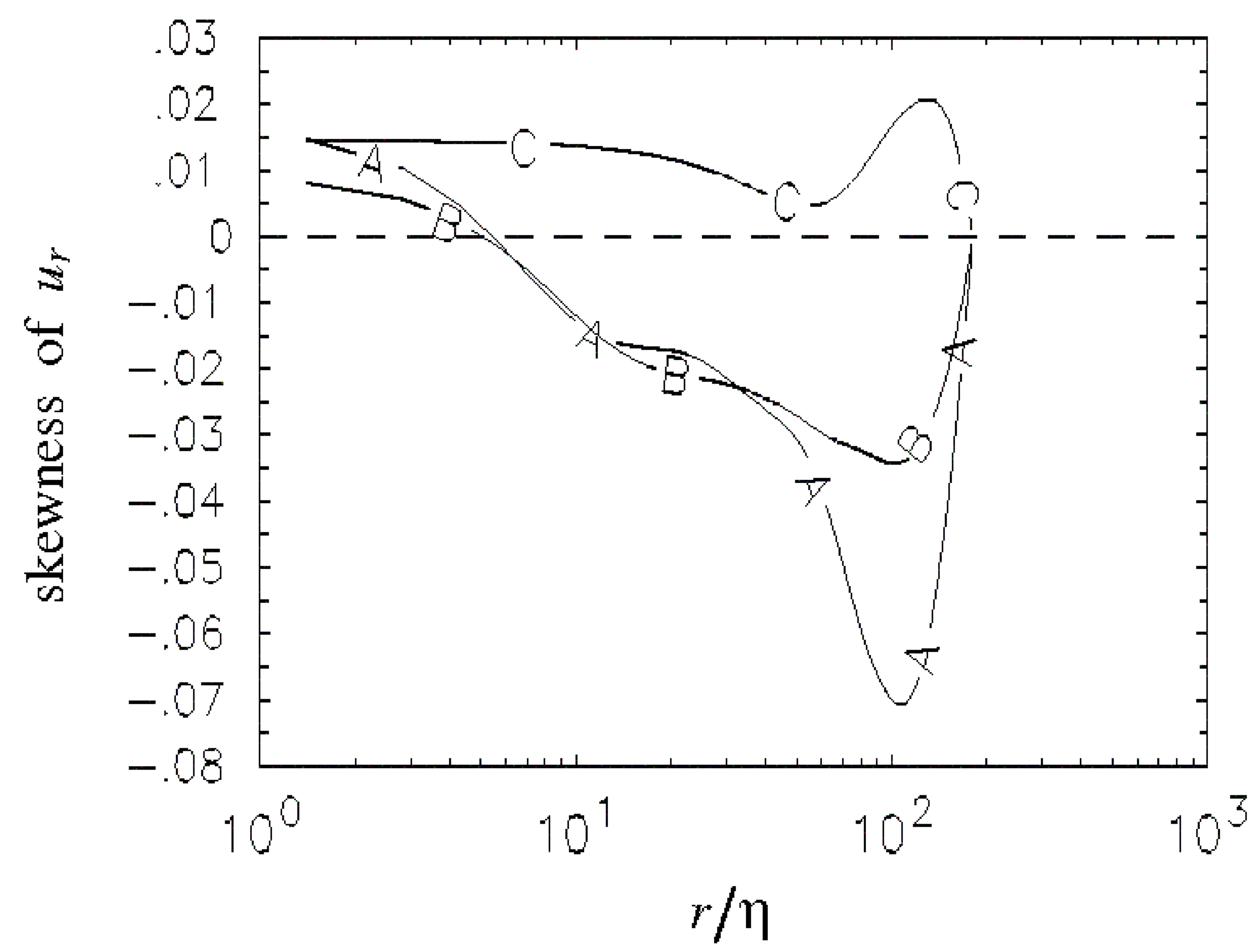

Figure 4. SKEWNESS OF LONGITUDINAL VELOCITY INCREMENT IN DIFFERENT DIRECTIONS, UNDER THE SAME CONDITIONS AS FIGURE 2.

isotropic conditions to study the effects of solid-body rotation on basic scaling properties of the velocity field in turbulent flow. Ensemble-averaged results at two different rotation rates indicate that at sufficiently high rotation rate the velocity fluctuations become slightly sub-Gaussian, longitudinal velocity gradients become essentially unskewed, and velocity gradients along the axis of rotation become Gaussian. Velocity gradient statistics show significant deviations from local isotropy. At the same time there is a reduced probability of rare events, an effect that is manifested also in the skewness and flatness factors of both the enstrophy and the energy dissipation rate. Velocity structure function are shown to deviate markedly from classical Kolmogorov theory, which must be modified to include the rotation rate as a basic parameter.

The results discussed above are only for one initial Reynolds number. Further simulations at higher grid resolution are necessary to obtain quantitative knowledge of dependence on both Reynolds number and Rossby number. Results on the effects of rotation on the scaling of passive scalar fluctuations and fluid particle motion in a Lagrangian frame are to be reported separately elsewhere.

ACKNOWLEDGMENT

The first and third authors acknowledge memories of pleasant past interactions with Professor Charles G. Speziale. This work is supported by NSF via Grants CTS-0121030 (PKY) and CTS-0121007 (KRS), as well as via NSF cooperative agreement ACI-9619020 through computing resources provided by the National Partnership for Advanced Computational Infrastructure at the San Diego Supercomputer Center.

REFERENCES

[1] C. Speziale. Turbulence modeling in non-inertial frames of refence. *Theor. Comput. Fluid Dyn.*, 1:3–xxx, 1989.

[2] Y. Zhou. A phenomenological treature of rotating turbulence. *Phys. Fluids*, 7:2092–2094, 1995.

[3] G. Bewley, P.K. Yeung, and K.R. Sreenivasan. Rotating turbulence: experiments and numerical simulation. *Bull. Am. Phys. Soc*, 47(10):112, 2002.

[4] P.K. Yeung and Y. Zhou. Numerical study of rotating turbulence with external forcing. *Phys. Fluids*, 10:2895–2909, 1998.

[5] Y. Morinishi, K. Nakabayashi, and S.Q. Ren. Dynamics of anisotropy on decaying homogeneous turbulence subjected to system rotation. *Phys. Fluids*, 13:2912–2922, 2001.

[6] J.A. Domaradzki and K. Horiuti. Similarity modeling on an expanded mesh applied to rotating turbulence. *Phys. Fluids*, 13:3510–3512, 2001.

[7] R.S. Rogallo. Numerical experiments in homogeneous turbulence. Technical report, NASA Ames Research Center, 1981.

[8] N.N. Mansour, C. Cambon, and C.G. Speziale. Theoretical and computational study of rotating isotropic turbulence. In T. Gatski, editor, *Studies in Turbulence*, pages 59–75, 1992.

[9] P.K. Yeung and Y. Zhou. On the universality of the kolmogorov constant in numerical simulations of turbulence. *Phys. Rev. E*, 56:1746–1752, 1997.

[10] K.R. Sreenivasan and R.A. Antonia. The phenomonlogy of small-scale turbulence. *Ann. Rev. Fluid Mech.*, 29:453–472, 1995.

[11] S. Chen, K.R. Sreenivasan, and M. Nelkin. Inertial range scalings of dissipation and enstrophy in isotropic turbulence. *Phys. Rev. Lett.*, 79:1253–1256, 1997.

[12] P.K. Yeung. Lagrangian characteristics of turbulence and scalar transport in direct numerical simulations. *J. Fluid Mech.*, 427:241–274, 2001.

[13] V.S. L'vov, E. Podivilov, and I. Procaccia. Invariants for correlations of velocity differences in turbulent fields. *Phys. Rev. Lett.*, 79:2050–2052, 1997.

[14] M. Nelkin. Enstrophy and dissipation must have the same scaling exponent in the high reynolds number limit of fluid turbulence. *Phys. Fluids*, 11:2202–2204, 1999.

[15] A.N. Kolmogorov. The local structure of turbulence in an incompressible fluid with very large reynolds numbers. *Dokl. Akad. Nauk SSSR*, 30:301–305, 1941.

[16] K.R. Sreenivasan. On the universality of the kolmogorov constant. *Phys. Fluids*, 7:2778–2784, 1995.